GASTROINTESTINAL, HEPATOBILIARY, AND PANCREATIC PATHOLOGY

Failure of Fibrotic Liver Regeneration in Mice Is Linked to a Severe Fibrogenic Response Driven by Hepatic Progenitor Cell Activation

Kaori Kuramitsu,* Deanna Y. Sverdlov,† Susan B. Liu,† Eva Csizmadia,* Linda Burkly,‡ Detlef Schuppan,† Douglas W. Hanto,* Leo E. Otterbein,* and Yury Popov†

From the Department of Surgery and the Division of Gastroenterology and Hepatology,† Beth Israel Deaconess Medical Center, Harvard Medical School, Boston; and Biogen Idec, Inc.,‡ Cambridge, Massachusetts*

Failure of fibrotic liver to regenerate after resection limits therapeutic options and increases demand for liver transplantation, representing a significant clinical problem. The mechanism underlying regenerative failure in fibrosis is poorly understood. Seventy percent partial hepatectomy (PHx) was performed in C57Bl/6 mice with or without carbon tetrachloride (CCl_4)-induced liver fibrosis. Liver function and regeneration was monitored at 1 to 14 days thereafter by assessing liver mass, alanine aminotransferase (ALT), mRNA expression, and histology. Progenitor (oval) cell mitogen tumor necrosis factor-like weak inducer of apoptosis (TWEAK) and TWEAK-neutralizing antibody were used to manipulate progenitor cell proliferation in vivo. In fibrotic liver, hepatocytes failed to replicate efficiently after PHx. Fibrotic livers showed late (day 5) peak of serum ALT (3542 ± 355 IU/L compared to 93 ± 65 IU/L in nonfibrotic livers), which coincided with progenitor cell expansion, increase in profibrogenic gene expression and de novo collagen deposition. In fibrotic mice, inhibition of progenitor activation using TWEAK-neutralizing antibody after PHx resulted in strongly down-regulated profibrogenic mRNA, reduced serum ALT levels and improved regeneration. Failure of hepatocyte-mediated regeneration in fibrotic liver triggers activation of the progenitor (oval) cell compartment and a severe fibrogenic response. Inhibition of progenitor cell proliferation using anti-TWEAK antibody prevents fibrogenic response and augments fibrotic liver regeneration. Targeting the fibrogenic progenitor response represents a promising strategy to improve hepatectomy outcomes in patients with liver fibrosis. *(Am J Pathol 2013, 183: 182−194; http://dx.doi.org/10.1016/j.ajpath.2013.03.018)*

The liver is the only organ that has the impressive ability to regenerate after injury or surgical resection.[1] Partial hepatectomy (PHx) is the most commonly used model for studying this unique capacity of the liver. After PHx, up to 95% of hepatocytes begin to replicate to compensate for the lost tissue and, in mice, regeneration reaches a maximum of 30 to 60 hours.[2] The remnant liver increases its volume until the regenerated liver mass approaches the original volume. This proliferation of hepatocytes is followed by proliferation of biliary epithelial cells and sinusoidal cells, and full restoration of hepatic architecture and function.[1]

The canals of Hering connect the terminal segment of the biliary ductal system with parenchymal hepatocytes.[3,4] Cells residing in the canals of Hering, called oval cells because of their morphology, function as adult hepatic stem cells. Oval cells express both fetal hepatocyte and biliary cell markers and have the ability to generate both hepatocytes and cholangiocytes,[5] thus considered to be bipotent progenitor cells in adult liver.[6]

Liver regeneration can occur via two distinct pathways, hepatocyte- and progenitor (oval) cell-mediated. After PHx performed on the healthy liver, hepatocytes are the primary replicating cells responsible for liver regeneration. Although contribution of intrahepatic and extrahepatic (bone marrow) stem cell was proposed, recent and carefully conducted cell fate-tracing studies confirm that normal liver regeneration occurs via mature hepatocyte proliferation.[7] Progenitor (oval) cell activation leading to hepatocyte regeneration is not observed during this process.[2,7] On the other hand, oval cell proliferation is prominent in some experimental models of liver injury and carcinogenesis induced by Azo dyes, choline deficient and ethionine-containing diets, D-galactosamine, acetylaminofluorene, or CCl_4 treatment.[8] When hepatectomy is combined with inhibition of mature hepatocyte replication, regeneration occurs primarily via the proliferation of oval cells and their differentiation into hepatocytes.[2]

The wound healing response is a series of cellular and molecular events necessary for prompt tissue repair after injury.[9] Chronic liver injury often results in hepatic fibrosis, defined by excessive extracellular matrix deposition in periportal areas or in the parenchyma that may progress to cirrhosis with distortion of hepatic architecture, compromised function, and life-threatening complications. Cirrhosis is common end-stage pathology of chronic liver disease of numerous etiologies. Although the mechanisms that lead to the progression of fibrosis, as well as the specific cells, mediators, and transcription factors that contribute to fibrosis progression are increasingly understood,[10] no clinically proven anti-fibrotic treatment exists.[11]

Hepatic resection is rarely performed in patients with liver cirrhosis, even of Child-Pugh grade A, due to poor outcomes. It is clinically well known that in the setting of advanced fibrosis, liver regeneration is severely impaired,[12] but a lack of mechanistic understanding of this phenomenon has severely hampered efforts to improve ability of fibrotic liver to regenerate and permit resection in these patients. To date, there is ample experimental literature focusing on liver regeneration after PHx in normal livers, but fibrotic liver regeneration remains understudied. Here, we describe the detailed characterization of a murine model of PHx of fibrotic liver, which permits further insights into molecular mechanisms of regeneration in the context of fibrotic liver and importantly allows formal preclinical testing of potential regeneration enhancing agents. We demonstrate for the first time that therapeutic targeting of the profibrogenic progenitor (oval) cell response offers a novel approach by which to improve regeneration in fibrotic livers.

Materials and Methods

Animal Experiments

All animal experiments and procedures were reviewed and approved by the Institutional Animal Care and Use Committee at Beth Israel Deaconess Medical Center (Harvard Medical School, Boston, MA; protocols #189-2006 and #158-2008). C57BL/6 mice (6-week-old males) were purchased from the Jackson Laboratory (Bar Harbor, ME) and used in experiments after 1 week of acclimatization in the animal facility at Beth Israel Deaconess Medical Center. CCl_4 and mineral oil were purchased from Sigma-Aldrich (St. Louis, MO). A 70% PHx was performed 3 days after the last dose of CCl_4 according to the standard procedure as previously described in mice,[13] with pre-established liver fibrosis induced ($n = 86$) or without ($n = 144$), described as follows. Briefly, anesthesia was induced by inhalation of isoflurane (2% v/v). After laparotomy, the left and median liver lobes were removed separately, distal to 4-0 silk ties. Body weights and the survival of each mouse were postoperatively recorded every day, and mice were sacrificed at selected time points after surgery.

Hepatotoxin-Induced Mouse Liver Fibrosis Model

Liver fibrosis was induced in C57Bl/6 mice (Jackson Laboratories, Bar Harbor, ME), according to an optimized escalating dose regimen of CCl_4 in mineral oil by oral gavage three times per week (Monday, Wednesday, and Friday) for 6 weeks, as previously established.[14] Nonfibrotic controls received mineral oil as a vehicle only.

Model of Liver Regeneration after PHx

Mice were sacrificed at 1, 2, 3, 5, 10, and 14 days after PHx to access liver regeneration parameters ($n = 10$ to 21 per time point), essentially as previously described.[15] Body weights at the time of sacrifice were measured, liver specimens and blood samples were collected, and liver weights were recorded. Resected liver tissues were immediately snap frozen in liquid nitrogen and were used as preresection controls to be compared to postresection parameters in each individual mouse. In initial experiments, both mineral oil-treated mice and untreated mice were used as normal controls (mineral oil-treated mice out of total per time point: day 1, 4 of 10; day 2, 8 of 16; day 3, 2 of 10; day 10, 6 of 16; day 14, 3 of 10). Because none of the general parameters differed among these control groups, as related to liver regeneration [body weight change after surgery, liver regeneration, hepatocyte proliferation, and alanine aminotransferase (ALT)] (levels of ALT, data not shown), the untreated mice were used as normal controls in all subsequent experiments.

Manipulation of Progenitor (Oval) Cell Compartment via the TWEAK Pathway

For progenitor (oval) cell inhibition experiments, mice were dosed intraperitoneally with either 75 µg neutralizing anti−tumor necrosis factor-like weak inducer of apoptosis (TWEAK) monoclonal antibody (clone P2D10, Biogen Idec, Cambridge, MA)[16] or 75 µg isotype IgG (mouse IgG2a, clone P1.17) generated from a commercial cell line (ATCC, Manassas, VA).

Oval cell proliferation was induced with recombinant TWEAK-Fc fusion protein (TWEAK-Fc, 75 μg per mouse).[16] All injections were made three times: on day 0 (4 hours after surgery), on day 2, and on day 4 after resection. All surviving mice were sacrificed and evaluated on day 5.

Assessment of Liver Regeneration

Liver regeneration ratio was calculated as the percentile of liver weight regained after PHx, as previously described.[15] Hepatocyte replication and oval cell proliferation were studied by immunohistochemistry (IHC). For the hepatocyte proliferation index, the number of total hepatocytes and Ki-67−positive hepatocytes were determined in each mouse liver by counting 10 random periportal fields at ×200 magnification, and calculating the percentage of replicating Ki-67−positive hepatocytes. Progenitor (oval) cell proliferation was assessed by the oval cell−specific marker A6.[17] Cells were counted in at least 10 random periportal fields at ×200 magnification for each mouse liver.

IHC and Immunofluorescence Staining

IHC, H&E, and connective tissue (Sirius Red) staining were performed in formalin-fixed, paraffin-embedded liver sections, as previously described.[18] The primary antibodies used in this study are summarized in Table 1. The A6 antibody was a kind gift from Dr. Valentina Factor (NIH, Bethesda, MD). Horseradish peroxidase−conjugated anti-rat or anti-rabbit antibodies were used for detection, and images were captured using Nikon light microscopy. For immunofluorescence staining, frozen liver tissues (5 μm thick) were cut and mounted on glass slides. Primary antibodies were visualized via conjugation to Alexa Fluor 488 and Alexa Fluor 592 antibodies (Molecular Probes, Life Technologies, Eugene, OR). Nuclei were counterstained blue with DAPI. Proliferation of oval cells was assessed by A6 and proliferating cell nuclear antigen (PCNA) double-immunofluorescence and double-positive cells were counted in randomly selected A6-reactive cell clusters at ×200 magnification in 4 to 5 fields per animal ($n = 5$). For florescence TUNEL staining, an apoptosis detection kit (Roche Diagnostics, Mannheim, Germany) was used by following the manufacturer's protocol. Images were documented with an Axiovert 200M Apotome wide-field microscope and Axiovision software version 4.6 (Zeiss, Thornwood, NY).

Table 1 List of Primary Antibodies for IHC and Immunofluorescence

Primary antibody	Type	Source
Ki-67 (clone TEC-3)	Rat monoclonal	Dako (Carpinteria, CA)
Phospho-histone3	Rabbit polyclonal	Cell Signaling (Danvers, MA)
A6	Rat monoclonal	Dr. Valentina Factor (NIH/NCl)
PCNA	Rabbit polyclonal	Santa Cruz Biotechnology (Dallas, TX)

PCNA, proliferating cell nuclear antigen.

Quantitative Real-Time RT-PCR

Relative mRNA levels were quantified in total liver RNA by real-time RT-PCR on a LightCycler 1.5 instrument (Roche Diagnostics) using the TaqMan methodology as we previously described in detail.[19] TaqMan probes (dual-labeled with 5′-FAM and 3′-TAMRA) and primers for major profibrogenic mRNA quantitation were previously designed and extensively validated.[14,19,20]

Hepatic Collagen Content

As a quantitative measure of fibrosis, hepatic collagen deposition was determined biochemically via relative hydroxyproline content (μg/g liver) in 250 to 300 mg liver samples from two different lobes after hydrolysis in 6N HCl for 16 hours at 110°C as previously described.[21] To assess collagen turnover in the settings of rapid liver mass changes during regeneration, total hepatic hydroxyproline (mg per whole liver) was calculated based on individual liver weights and the corresponding relative hydroxyproline content as previously described.[14,18] Total collagen content in remnant lobes liver at the time of surgery (day 0) was calculated by multiplying relative hydroxyproline content determined in removed lobes during hepatectomy by the weight of the remnant liver estimated from the weight of removed lobes (based on the assumption that 70% of the liver is removed and 30% remains). Thereafter, collagen changes were assayed directly in remnant regenerating liver by determining relative hydroxyproline in 200 to 300 mg sample, and multiplied by remnant weight to determine total hydroxyproline (ug per liver).

Serum levels of transforming growth factor beta (TGFβ)1 were assayed using eBioscience Human/Mouse TGF beta1 ELISA kit (#88-8350, eBioscience Inc., San Diego, CA) according to the manufacturer's instructions following additional centrifugation at $10,000 \times g$ for 10 minutes at 4°C to remove platelets.

Statistical Analysis

Results are expressed at means ± SEM. Statistical analyses were performed using the Student's *t*-test, and P values < 0.05 were considered significant. Survival data were analyzed using Kaplan-Meier estimates, and two-way analysis of variance was performed for the comparison between the two groups in the time course.

Results

Impaired Liver Regeneration and Poor Survival after 70% Hepatectomy in Mice with Pre-Established Experimental Liver Fibrosis

After 6 weeks of CCl₄ administration, all mice developed robust liver fibrosis. Total hepatic collagen content increased fourfold compared to control livers (Figure 1A)

($P < 0.001$), and the degree of fibrosis was characterized as intermediate, based on histological assessment (equivalent to Metavir score F2/F3) (Figure 1B). Three days after the last CCl_4 injection, a 70% PHx was performed and general physiological parameters (survival rate, body weight change, and percentage of regenerated liver weight) were compared between fibrotic mice and nonfibrotic controls. After hepatectomy, 90.8% of all nonfibrotic mice survived the surgery, whereas mice with ongoing fibrosis showed a significantly reduced survival rate (68.9%; $P < 0.05$) (Figure 1C). Fatalities in nonfibrotic mice were earlier (days 1 to 3) than in fibrotic mice (days 3 to 6) after hepatectomy, suggesting that mortality in the fibrotic group was related to compromised liver regeneration rather than to surgical complications. Nonfibrotic mice lost weight steadily after PHx from day 1, peaking at day 3 ($-12.4 \pm 4.6\%$), whereas fibrotic mice lost more weight over a longer period of time, peaking at day 4 ($-19.3 \pm 8.3\%$; $P < 0.001$) (Figure 1D).

To assess liver regeneration, we monitored restoration of liver weight at various time points after resection. As expected, nonfibrotic PHx mouse liver restored to original weight (38% increase at day 10 compared to day 1). In comparison, the liver weights in fibrotic PHx mice increased by only 11% at day 10 compared to day 1 (Figure 1E) ($P < 0.001$). These findings suggest that liver regeneration in fibrotic mice was severely compromised, even before cirrhosis is established, closely resembling the poor postresection outcomes in patients with advanced liver fibrosis and cirrhosis.[12]

Massive Hepatocyte Death during Liver Regeneration and Failure of Efficient Hepatocyte Replication in Fibrotic Mice after Hepatectomy

Next, we aimed to characterize the sequence of events responsible for deficient liver regeneration in the context of liver fibrosis. PHx induced a sharp increase in serum ALT at postoperative day 1 in both normal and fibrotic mice, but fibrotic mice showed a greater increase (1530 ± 107 IU/L in fibrotic versus 693 ± 166 IU/L in nonfibrotic mice, $P < 0.05$). Additionally, fibrotic mice showed a second, unexpected peak in ALT levels in the late recovery phase between days 4 and 6, peaking on day 5 (3542 ± 246 IU/L versus 93 ± 65 IU/L in nonfibrotic controls, $P < 0.0001$) (Figure 2A). Accordingly, serum AST, alkaline phosphatase, and total bilirubin increased in normal mice only transiently at 1 day, but peaked in fibrotic mice at a late day 5 time point and remained elevated at day 10 (Supplemental Table S1). Careful histological examination revealed that at postoperative day 5, 71% of fibrotic mice showed focal eosinophilic lesions in the periportal area consisting of large numbers of dead hepatocytes not found in the fibrotic livers at earlier (days 1 to 3) or later (days 10 to 14) time points and at no point in regenerating nonfibrotic livers (Figure 2C). TUNEL staining revealed a high rate of cell apoptosis, predominantly localizing to areas of focal hepatocyte death, suggesting that hepatocyte cell death occurred via apoptosis (Figure 2C). In fibrotic livers before PHx, TUNEL$^+$ cells were observed in fewer numbers and localized within portal tracts and fibrotic septa (Figure 2D), whereas normal livers were virtually TUNEL negative before and 5 days after hepatectomy. No cholangiocyte death could be detected histologically (neither in bile ducts nor pseudo ducts of normal or fibrotic mice, not shown).

After 70% PHx in nonfibrotic livers, organ volume and function was quickly restored via robust replication of almost all mature hepatocytes, as assessed by immunostaining of liver sections for the nuclear proliferation marker Ki-67. In normal livers before surgery, hepatocytes were quiescent. After PHx, hepatocytes began to proliferate, peaking at day 2 postsurgery (79% Ki-67$^+$ hepatocytes) (Figure 2, B and E). As expected in fibrotic livers, the baseline hepatocyte proliferation was elevated before PHx due to ongoing chronic liver injury and hepatocyte regeneration. However, Ki-67 staining in livers of fibrotic mice was severely blunted with only 1.8% and 10.5% of hepatocytes proliferating on days 2 and 3, respectively, compared with 7.3% and 79.1% in normal mice ($P < 0.05$) (Figure 2, B and E). Moreover, the rate of Ki-67–positive hepatocytes failed to increase at later time points (Figure 2B). These findings suggest that in the context of the fibrotic microenvironment, liver regeneration after PHx is severely compromised, primarily by the failure of hepatocyte replication in early states (days 1 to 3), followed by massive focal hepatocyte death at day 5.

Activation of Adult Hepatic Progenitor (Oval) Cells Follows the Failure of Hepatocyte-Mediated Regeneration in Fibrotic Liver

When hepatocyte replication is inhibited during regeneration after PHx, the liver restores its mass via the alternative pathway of adult hepatic progenitor (oval) cell activation.[2] We hypothesized that failure of hepatocyte replication and increased cell death after PHx in fibrotic livers may elicit a similar progenitor response, and analyzed the oval cell compartment using the progenitor (oval) cell marker A6. In normal livers, A6-positive staining was observed only within the portal tracts in quiescent (before PHx) and proliferating bile ducts (days 5 and 10 post-PHx). In fibrotic mice before resection, the number of A6-positive cells was markedly increased and could be observed both in the portal area and within fibrotic septa extending into the lobule. After PHx in fibrotic mice, the percentage of A6-positive cells further increased dramatically from day 5 and peaked at day 10 (threefold increase compared to pre-PHx level and 14-fold increase compared to normal liver (Figure 3A and B) ($P < 0.05$) at days 5 and 10 versus normal liver, returning to pre-PHx levels by day 14. The staining pattern of A6 was associated with scattered spindle-shaped cells and irregular-shaped bile duct-like proliferations (Figure 3A), characteristic of the pseudoducts formed by proliferating progenitor (oval) cells. These cells also stained positive for the alternative progenitor marker pan-cytokeratin (not shown). Sham surgery alone did

not elicit progenitor response (Supplemental Figure S1). Interestingly, increase in circulating TGFβ1 levels in fibrotic (but not normal) mice serum coincided with hepatocyte death and progenitor (oval) cell expansion at 5 days (Figure 3C). Evidently, the expansion of progenitor (oval) cells in fibrotic livers occurred via active proliferation, because nuclei of A6-immunoreactive progenitor cells were frequently positive for the proliferation marker PCNA, as demonstrated by double-immunostaining (Figure 3D). At day 5 post-PHx, at least one PCNA-positive nucleus was detectable in 52% of randomly selected A6-reactive cell clusters, with an average of 9.93 ± 2.3% PCNA-positive cells in A6-positive cell population.

Compromised Fibrotic Liver Regeneration Is Associated with Increases in Profibrogenic mRNA Expression and *de Novo* Collagen Synthesis and Deposition

Given that the mobilization of hepatic progenitors is clinically associated with progressive liver fibrosis,[22,23] we determined collagen deposition and profibrogenic gene expression in fibrotic livers after PHx. Histological examination of liver sections at late regeneration (day 10) in mice with pre-existing fibrosis suggested active collagen deposition around the proliferating ductular structures with irregular shape (Figure 4A) that stained positive for A6 (pseudoducts). To quantitatively assess the activity of fibrogenesis during liver regeneration, we measured transcript levels of several well established fibrogenesis activity markers, including TGFβ1, procollagen α 1(I), α-smooth muscle actin (α-SMA), and tissue inhibitor of metalloproteinases-1 (TIMP-1). All of these markers increased several-fold and peaked at day 5, whereas nonfibrotic mice showed low profibrogenic mRNA levels throughout regeneration after PHx (Figure 4B). Interestingly, this dramatic increase in profibrogenic transcripts, which can be ascribed mainly to activated hepatic stellate cells and myofibroblasts, coincided with a similar increase in TGFβ2 and integrin β6 (Figure 4B). Both molecules are expressed specifically by activated biliary epithelium (reactive cholangiocytes and progenitor cells) in liver fibrosis,[20]
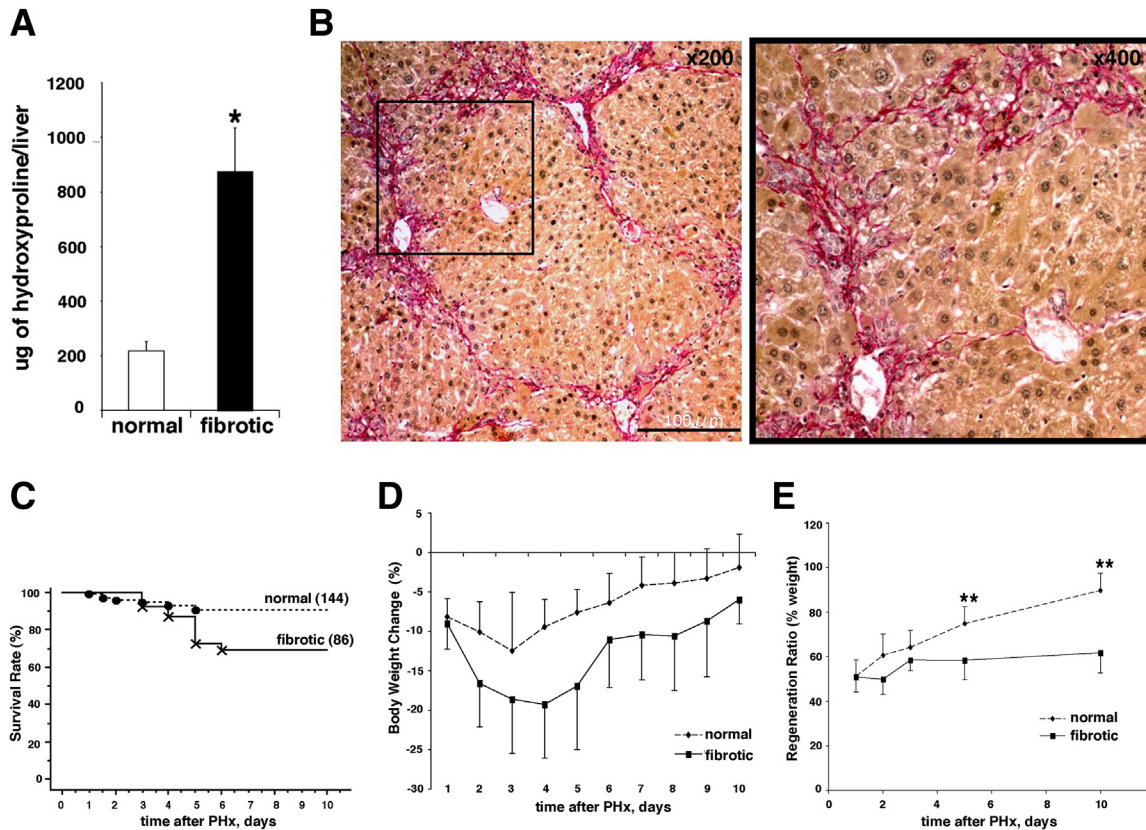

Figure 1   Impaired liver regeneration in fibrotic mice, as measured by survival rate, body weight, and restoration of liver volume after PHx. **A:** Robust liver fibrosis was induced by chronic CCl₄ injections for 6 weeks, leading to a fourfold increase in total hepatic collagen content (μg per liver) in mice receiving CCl₄ via oral gavage. *$P < 0.001$ versus normal mice receiving mineral oil only. **B:** Connective tissue staining (Sirius red) showing histological signs of early bridging fibrosis. Scale bar = 200 μm. Original magnification: ×100 (**left panel**); ×200 (**right panel**). **C:** Reduced survival in mice with pre-established liver fibrosis after 70% PHx. Survival rate was calculated using the Kaplan-Meier method and was 90.8% in normal mice (137 of 144) compared to 68.9% in fibrotic mice (70 of 86. $P < 0.05$ versus normal mice. **D:** Loss of body weight after hepatectomy is more significant in fibrotic mice after PHx. $P < 0.05$ versus normal mice. Each mouse was weighed every day until day 10 post-PHx, results represent percent change in individual mouse body weight versus body weight before hepatectomy (means ± SEM). **E:** Restoration of liver volume is compromised in fibrotic livers. Regeneration ratio was assessed by dividing each regenerated liver weight at sacrifice by the estimated remnant liver weight, as described in *Materials and Methods*. Data are expressed as means ± SEM (6 to 12 mice per group), as described in *Materials and Methods*. **$P < 0.0001$ compared to normal mice at corresponding time points.
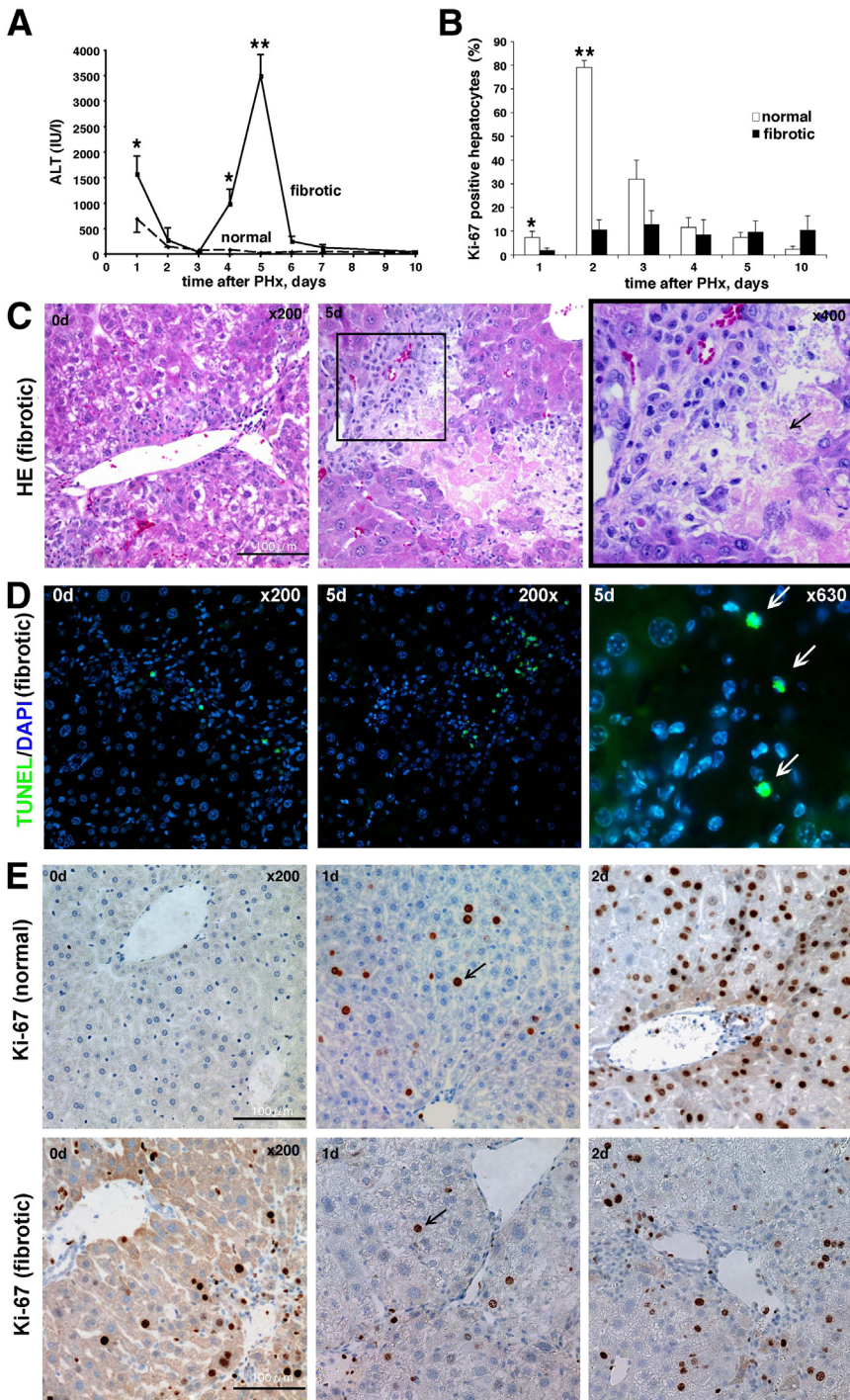
Figure 2 Repressed hepatocyte replication and increased hepatocyte cell death in fibrotic mice after PHx. **A:** Marked increase in serum transaminases at late stages (4 to 6 days) after PHx suggests massive hepatocyte death in mice with pre-established fibrosis. Serum ALT levels were monitored over time in normal and fibrotic mice after PHx. Means ± SEM (*n* = 6 to 12 mice per group). *$P < 0.01$ at day 1 and **$P < 0.0001$ at day 5 versus normal mice. **B:** Quantification of Ki-67+ nuclei of hepatocytes after PHx. Hepatocytes were identified by typical morphological appearance and Ki-67+ nuclei were counted in 10 high-power fields in at least five individual mice per time point. Each bar represents means ± SEM of the number of positive hepatocytes and high-power field. *$P < 0.05$, **$P < 0.0001$ versus normal mice. **C:** H&E staining of liver samples at selected time points after hepatectomy. **Arrow** indicates eosinophilic area of vanishing dead hepatocytes in periportal areas. Original magnification: ×200 (left and middle); ×400 (right). Scale bar = 200 μm. **Left image,** day 0; **middle** and **right images,** day 5. **D:** TUNEL staining notably increased at day 5 after PHx in fibrotic livers. and localize within and at the interface areas of hepatocytic death (**arrows**), suggesting apoptotic cell death mechanism. **E:** Hepatocytes in fibrotic mice fail to replicate after PHx. Representative images from liver sections stained with proliferation marker Ki-67 show low replicative activity in hepatocytes in fibrotic (**upper row**) versus nonfibrotic livers (**lower row**) at day 2 after hepatectomy. **Arrows** indicate positive Ki-67 staining in hepatocyte nuclei. Scale bar = 100 μm.

cells that are considered major drivers of biliary-type fibrosis.[11,20,24]

Next, we aimed to determine whether increased profibrogenic mRNA resulted in collagen synthesis and deposition, and we analyzed the quantitative changes in hepatic collagen protein content after PHx in mice with pre-existing fibrosis. Because significant changes in liver mass may occur rapidly compared to the relatively slow process of fibrotic tissue deposition, total collagen content (per whole organ) was measured in addition to relative collagen levels (μg/100 mg of tissue) to accurately assess changes in fibrotic liver.[14,18] Collagen quantitation in resected lobes and in the regenerating remnant liver revealed two things: a drop in relative hydroxyproline level by 44% at day 1 (reflecting dilution of fibrous tissue due to rapid gain in liver volume), which increased again starting at day 5 to almost the pre-PHx levels (71% and 88% of average pre-PHx values at days 5 and 10, respectively) ($P < 0.05$); and no
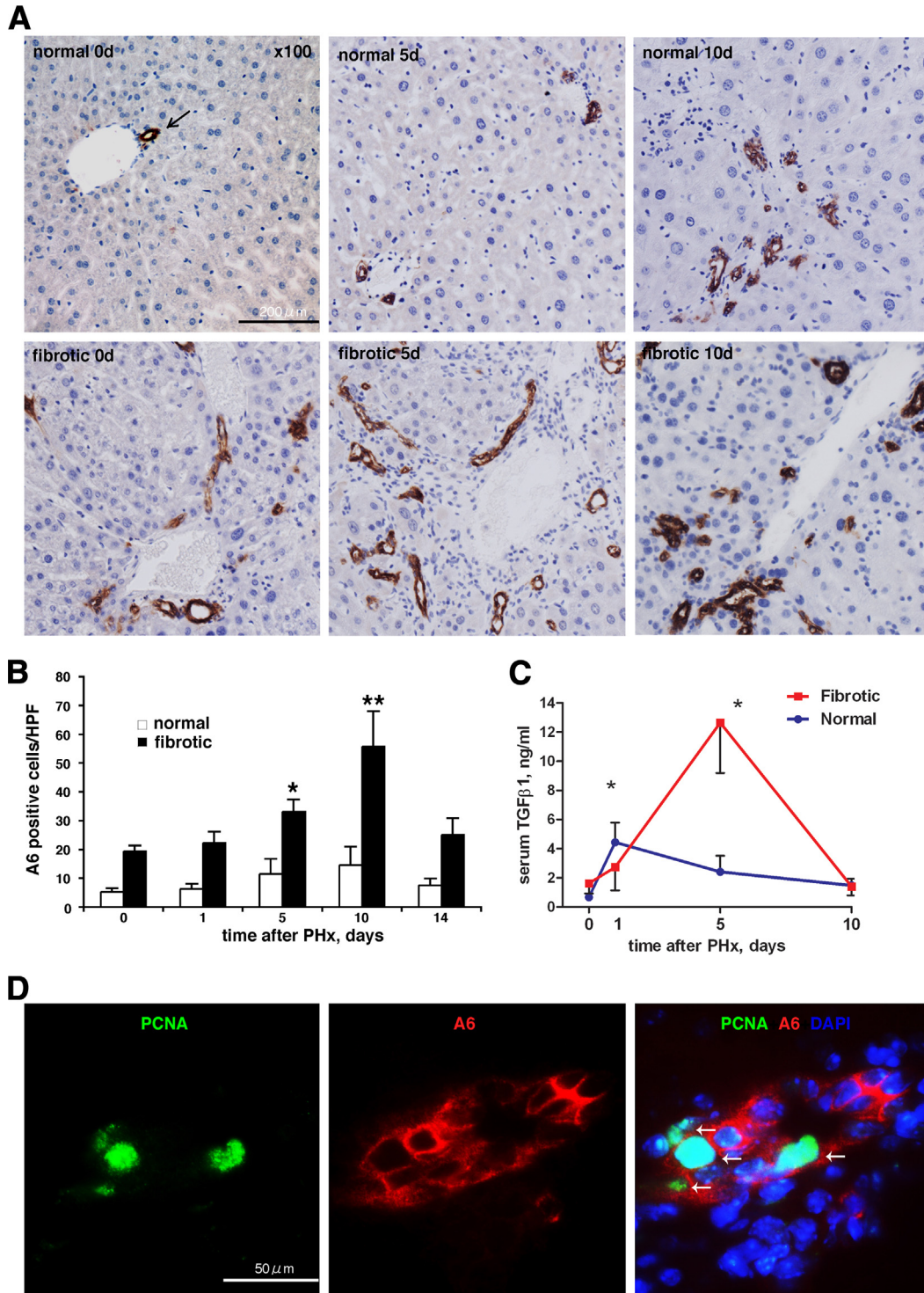
Figure 3 Massive activation of hepatic progenitor (oval) cell compartment in late stages of regeneration in fibrotic livers. **A:** Expansion of hepatic progenitor (oval) cells in portal areas starting from day 5 after PHx in fibrotic liver. Representative images from liver sections stained for oval cell marker A6 at selected time points in normal and fibrotic mice after hepatectomy. **Upper panel:** Normal liver without hepatectomy at days 0, 5, and 10 after PHx. **Lower panel:** Fibrotic liver at 0, 5, and 10 days after hepatectomy. **Arrow** indicates positive staining. Original magnification, ×100. Scale bar = 200 μm. **B:** Quantification of A6$^+$ oval cells numbers after PHx in normal (open bars) versus fibrotic (closed bars). Ten randomly chosen portal vein areas were assessed in sections from five individual mice (means ± SEM of A6$^+$ cell counts per high-power fields). *$P < 0.001$, **$P < 0.0001$ versus livers without hepatectomy. **C:** Serum TGFβ1 levels after PHx differ significantly in normal and fibrotic mice and increase dramatically at day 5 in fibrotic mice. Serum TGFβ1 was determined using an eBioscience Human/Mouse TGF beta1 ELISA kit , as described in *Materials and Methods*. **D:** A6$^+$ progenitor (oval) cells actively proliferate in fibrotic liver after hepatectomy. Representative image is shown (5 days post-PHx, fibrotic) of double-immunofluorescence staining of liver samples for progenitor cell and proliferation markers that frequently colocalize (**arrows**). PCNA, green, nuclear proliferation marker; A6, red, cytoplasmic oval cell marker; DAPI, blue, nuclei. Original magnification, ×200. Scale bar = 50 μm.
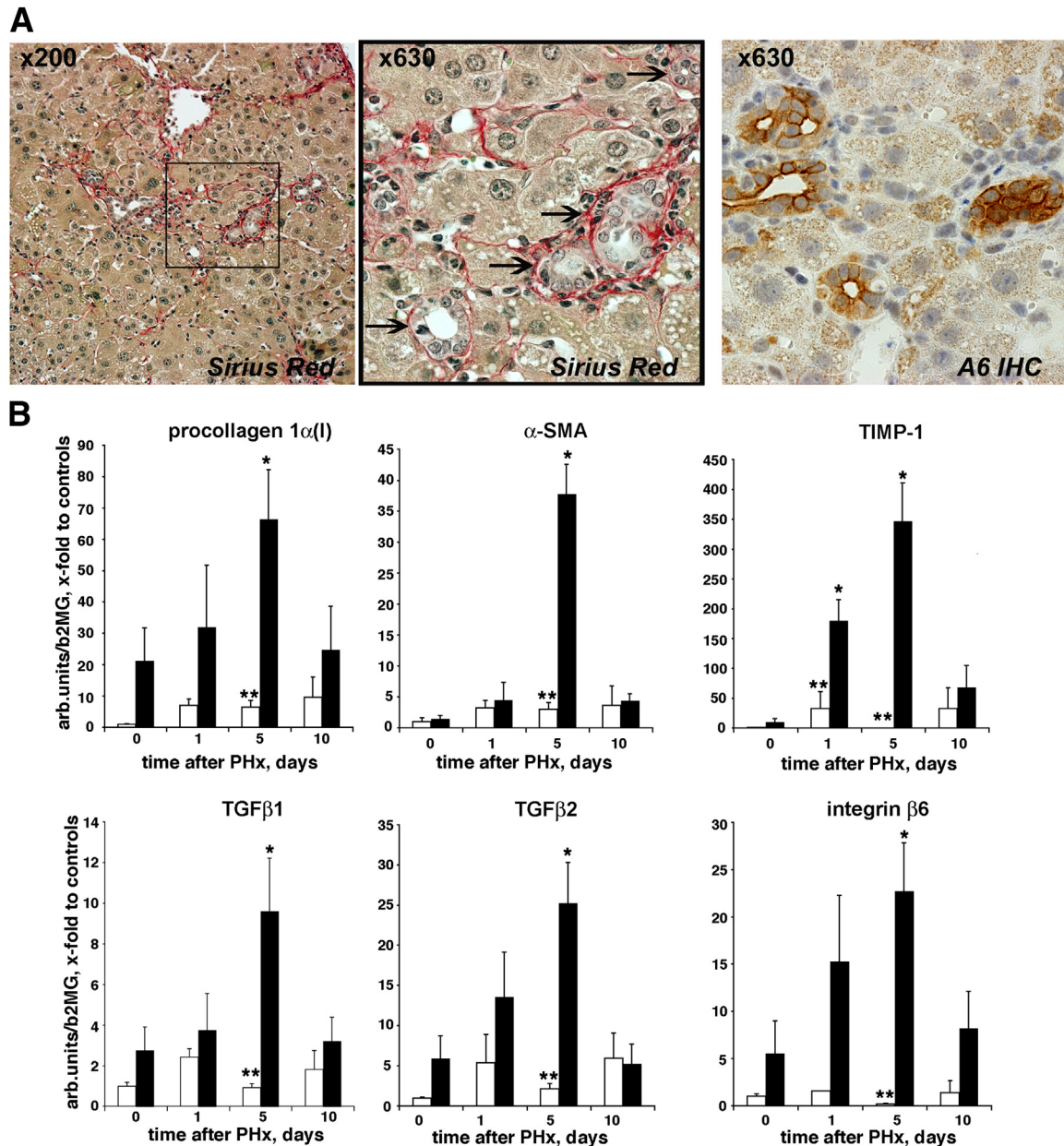
Figure 4 PHx elicits delayed, additive profibrogenic response in fibrotic mice. **A:** Connective tissue staining (Sirius Red) demonstrates reactive collagen deposition around duct-like proliferations (**arrows**). Representative liver section of fibrotic mice 10 days after PHx. Oval cell marker A6 staining labels these ductular structures of the same area. **B:** Dramatic increase in profibrogenic expression which peaks 5 days after PHx in regenerating fibrotic liver (black bars) but not in normal liver (white bars). Liver samples were collected at selected time points after hepatectomy, and hepatic mRNA levels of procollagen α1(I) (collagen), α-SMA, TIMP-1, TGFβ1, and TGFβ2, and integrin β6 were analyzed by real-time PCR. Results represent means ± SEM expressed as fold change over normal mouse controls from 4 to 6 mice per group. *$P < 0.05$ versus fibrotic livers before hepatectomy; **$P < 0.05$ versus normal liver at corresponding time points.

change in total collagen content in the remaining lobe at day 1, but a significant increase starting from day 5 (reaching 133% and 160% of average pre-PHx values at days 5 and 10, respectively) ($P < 0.05$), as summarized in Table 2. This indicates that the profibrogenic response at day 5 resulted in *de novo* collagen synthesis and deposition. The fibrogenic process triggered by PHx can be defined as severe, because the actual rate of collagen deposition during regeneration (average 15.41 μg of hydroxyproline per day per liver) is comparable to the most aggressive

CCl₄-induced fibrosis[14] (average 15.24 μg of hydroxyproline per day per liver, assuming that collagen deposition is a linear process) (Figure 1A). In contrast, total collagen content increased only modestly, and relative collagen content remained below pre-hepatectomy levels in normal mice (Table 2). These findings suggest that activation of oval cell-mediated regeneration in fibrotic livers is associated with a pronounced fibrogenic response comparable to levels during active chronic fibrosis. This in turn results in rapid *de novo* deposition of fibrotic tissue in the remnant

Table 2 Collagen Content Increases in the Remnant Liver after 70% PHx in Fibrotic Mice, Indicating Active Fibrogenesis and *de Novo* Collagen Deposition

Groups	Relative collagen content (µg/100 mg)		Total collagen content (µg/liver)	
	Before surgery*	After 70% PHx	Before surgery[†]	After 70% PHx
Day 1 (F)	50.98 ± 4.64	28.84 ± 3.1[‡]	236.7 ± 14.51	229.2 ± 26.35
Day 5 (F)	51.32 ± 2.64	36.40 ± 3.34[‡]	251.1 ± 17.66	334.7 ± 18.83[‡]
Day 10 (F)	49.97 ± 4.75	43.79 ± 6.46	259.0 ± 31.37	413.1 ± 30.45[‡]
Day 1 (N)	18.01 ± 0.44	13.22 ± 0.68[‡]	63.46 ± 2.75	75.89 ± 4.55
Day 5 (N)	18.13 ± 0.34	11.78 ± 0.32[‡]	65.35 ± 3.4	103.9 ± 5.07[‡]
Day 10 (N)	18.73 ± 0.51	13.54 ± 0.78[‡]	65.44 ± 2.6	150.6 ± 11.04[‡]

Collagen content was determined biochemically via hepatic hydroxyproline in the resected lobe of each individual mouse at the time of surgery and in the remnant liver after regeneration for 1, 5, and 10 days ($n = 6$ to 8 per group). Both relative (per 100 mg of liver) and total collagen content (per whole remaining liver) increased significantly starting from day 5 in fibrotic mice (F), suggesting significant *de novo* collagen synthesis and deposition occurs after partial hepatectomy (PHx) in mice with pre-existing fibrosis. In normal mice (N) relative collagen remained below pre-PHx levels up to day 10, whereas total collagen in remnant liver increased modestly.

*Relative collagen levels determined in removed 70% of the liver at the time of surgery (day 0).

[†]Estimated in remaining 30% of liver based on corresponding values in resected lobes.

[‡]$P < 0.05$ compared to pre-PHx levels in corresponding group (Student's *t*-test).

liver after PHx, which is likely to further impair hepatic regeneration.

Manipulation of Hepatic Progenitor Cells Modulates the Profibrogenic Response and Fibrotic Liver Regeneration *in Vivo*

Our findings thus far have suggested that oval cell-mediated liver regeneration is activated in fibrotic mice, and progenitor cell expansion is spatiotemporally associated with adverse events during impaired regeneration of the fibrotic liver, including an increase in serum ALT and amplified fibrogenesis. To test whether activation of the progenitor cell compartment modulates fibrotic liver regeneration and clinical outcomes after resection, we took advantage of the recently identified TWEAK pathway to experimentally manipulate the mitogenic oval cell response.[25,26] We treated fibrotic mice after 70% hepatectomy with either the oval cell mitogen TWEAK administered exogenously to amplify the progenitor response, or TWEAK-neutralizing antibody to inhibit the progenitor reaction. We evaluated parameters of regeneration, liver function, and fibrogenesis 5 days post-resection, when most of the adverse changes in fibrotic mice peaked. Histological examination revealed significant expansion of duct-like structures positive for the oval-cell marker A6 in the TWEAK-treated group. Conversely, progenitor (oval) cell proliferation was dramatically reduced in the group that received TWEAK-neutralizing antibody (Figure 5A). Furthermore, profibrogenic gene expression was significantly down-regulated at day 5 for all studied mRNAs (TGFβ1, procollagen I, α-SMA, TIMP-1, TGFβ2, integrin β6) in the group treated with anti-TWEAK mono-colonal antibody (Figure 5D). Moreover, regeneration ratio was improved and serum ALT levels were normalized in the anti-TWEAK group ($P < 0.05$) compared to the isotype controls (Table 3 and Supplemental Table S2). The group

treated with anti-TWEAK antibody also showed an early trend to lower relative hepatic collagen levels at 5 days and histologically less severe fibrosis (Table 3 and Figure 5B). In contrast, mice treated with the oval cell mitogen TWEAK showed significantly upregulated procollagen I, TGFβ2, and integrin β6 transcripts, whereas TGFβ1, α-SMA, and TIMP-1 remained elevated and did not change compared to the isotype antibody controls. Serum ALT was not changed by exogenous TWEAK treatment. Importantly, blocking TWEAK by antibody stimulated hepatocyte replication (by 85% compared to isotype controls ($P = 0.0013$) (Figure 5C and Table 3), whereas administration of TWEAK resulted in predominant replication of progenitor (oval) cells within ductular structures (Figure 5C and Table 3). Taken together, these data indicate that activation of the progenitor (oval) cell compartment not only coincides with the failure of fibrotic liver regeneration, but also contributes functionally to it, via amplification of the profibrogenic response after resection.

Discussion

Rigorous mechanistic understanding of the failure of fibrotic liver to regenerate (as opposed to the almost unlimited regenerative capacity of normal livers) is critical toward the development of safe and targeted ways to improve liver resection outcomes in patients with chronic liver disease and cirrhosis. Although normal liver regeneration has been extensively studied for the past few decades, surprisingly little is known about the pathophysiology of fibrotic liver regeneration.

Here, we performed a comprehensive characterization of liver regeneration after 70% partial hepatectomy in normal mice and those with pre-established experimental fibrosis. This analysis revealed profound, characteristic, and in some instances even unexpected differences between regeneration on normal and fibrotic livers that can explain much of the
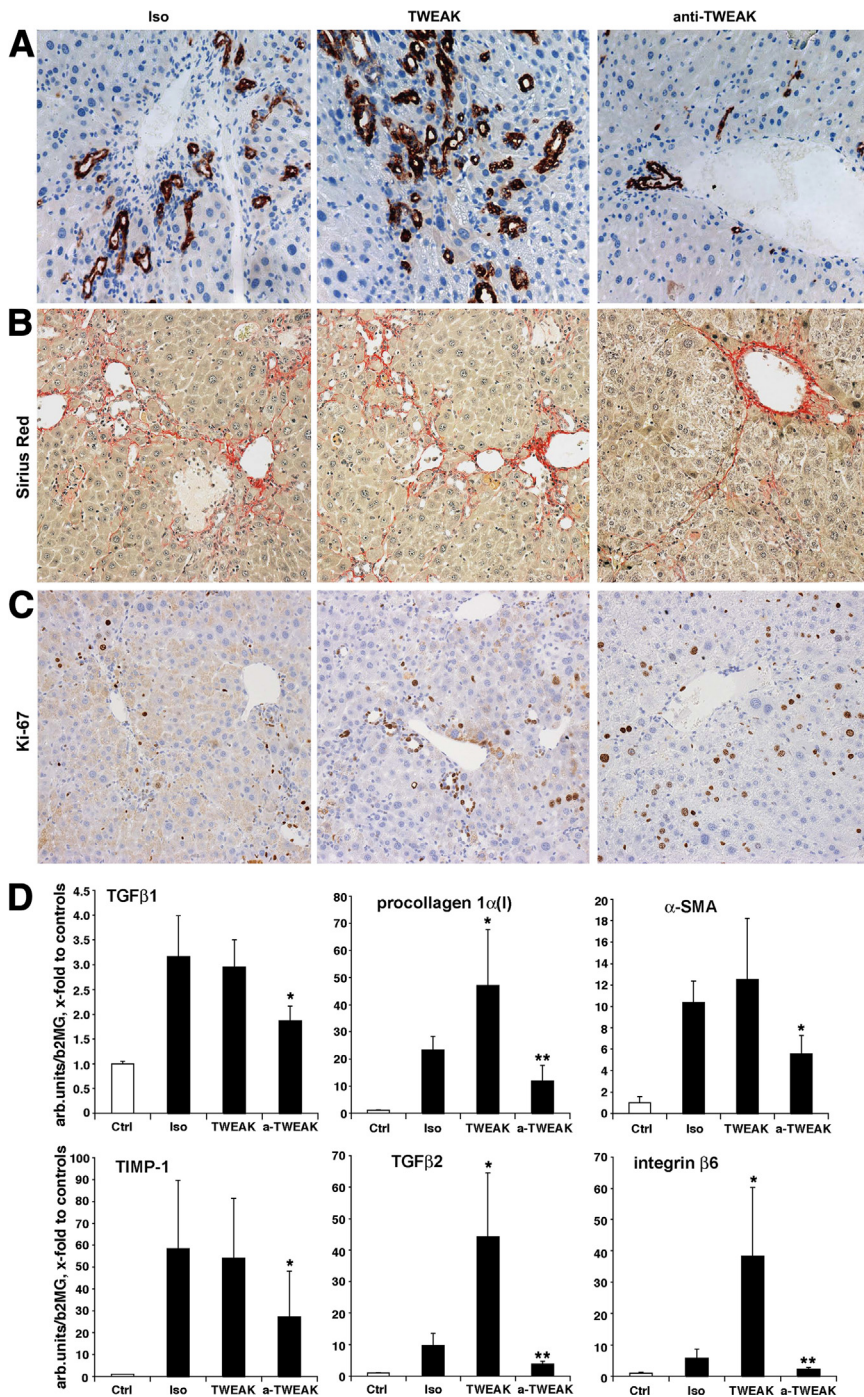
Figure 5 Manipulation of hepatic progenitor expansion during regeneration modulates fibrogenic response and fibrotic liver regeneration. Experimental manipulation of the hepatic progenitor (oval) cell proliferative response post-PHx was effectively achieved in both directions: robust increase in A6$^+$ progenitor cells in animals receiving TWEAK-Fc injections (TWEAK, 75 μg per mouse, $n = 10$), as well as dramatic inhibition of the oval cell response in mice receiving neutralizing anti-TWEAK antibody (α-TWEAK, 75 μg per mouse, $n = 6$) compared to mice injected with irrelevant isotype IgG (P1.17, 75 μg per mouse, $n = 8$). **A:** Representative images from liver sections stained with oval cell marker A6 IHC in fibrotic mice at day 5 after PHx. Connective tissue (Sirius Red) staining (**B**) and proliferation marker (Ki-67) IHC (**C**) of livers from fibrotic mice treated with isotype control antibody (Iso), TWEAK-Fc (TWEAK), or anti-TWEAK antibody (anti-TWEAK) 5 days after 70% PHx. Note increased proliferation predominantly of hepatocytes in anti-TWEAK group and mostly within ductular structures in TWEAK-treated mice (quantified in Table 3). **C:** Representative images shown. Original magnification, ×200. **D:** Manipulation of oval cell proliferation modulates profibrogenic response associated with fibrotic liver regeneration. Significant decrease in profibrogenic mRNA expression 5 days after PHx in mice receiving TWEAK-neutralizing antibody (anti-TWEAK, 75 μg per mouse). Hepatic mRNA level of TGFβ1, COL1A1 (procollagen type 1), α-SMA, TIMP-1, TGFβ2, and integrin β6 were analyzed by real-time RT-PCR. Each bar represents means ± SEM expressed as fold change over normal controls ($n = 6$ to 8 per group). *$P < 0.05$, **$P < 0.01$ compared to isotype control group (P1.17).

compromised, pathological regeneration of the fibrotic liver. In striking contrast to normal liver regeneration, fibrotic liver showed: i) failure of appropriate parenchymal cell replication, as evidenced by an eightfold lower rate of hepatocytes positive for proliferation markers; ii) significant cell death in late stages of regeneration (peak at day 5) as demonstrated by focal hepatocyte apoptotic cell death and increased ALT levels; iii) an association with a marked progenitor (oval) cell expansion, as evidenced by a 14-fold increase in A6-positive cells at day 10; and iv) a severe

fibrogenic response, as reflected by a dramatic upregulation of multiple profibrogenic genes resulting in further excess collagen deposition. We propose that these pathophysiological features comprise the pathological sequence of events that lead to impaired restoration of liver volume and function in hepatectomized fibrotic mice.

Impairment of hepatocyte replication after PHx in the fibrotic rat liver was described earlier, consistent with our findings (Figure 2E), and proposed to be linked to a failure of cyclin D induction.[27] Accordingly, stimulation of hepatocyte

Table 3 Liver Regeneration, Serum ALT, and Hepatic Hydroxyproline Levels in Fibrotic Mice Treated with TWEAK and Anti-TWEAK after 70% Hepatectomy

Group	Regeneration ratio (%)	ALT (U/L)	Collagen (ug/100 mg)	Proliferation (Ki-67+ cells/ high-power fields)	
				Hepatocytes	Ductular cells
P1.71	49.69 ± 4.54	306 ± 88	41.14 ± 3.05	9.66 ± 0.87	10.33 ± 1.24
TWEAK	50.80 ± 4.74	153.6 ± 60.6	44.50 ± 2.85	9.15 ± 1.21	24.47 ± 2.88*
Anti-TWEAK	62.89 ± 2.58*	48.5 ± 23.3*	33.95 ± 2.35	17.76 ± 1.14*	3.80 ± 0.29*

Regeneration ratio was assessed by calculating each regenerated liver weight at the time of sacrifice (day 5) as percentage of pre-resection liver weight (estimated based on weight of resected lobes). Serum alanine aminotransferase (ALT) levels and hepatic collagen (as hydroxyproline content) were measured at sacrifice, as described in *Materials and Methods* (n = 6 to 10 mice per group). Cell proliferation was assessed by quantification of Ki-67+ hepatocytes and Ki-67+ ductular cells (see staining in Figure 5, C and D). Ten random high-power fields at ×200 magnification were counted in 4 to 5 mice per group. Data are expressed as means ± SEM.

*P < 0.05 versus P1.71 control group.

replication with hepatocyte growth factor gene therapy accelerated regeneration after hepatectomy in fibrotic liver.[28] However, focal hepatocyte cell death with a marked increase in serum transaminase levels at late stages of regeneration (days 4 to 6) in fibrotic liver (Figure 2, A and C) has not been described before and appears to be relevant to the increased mortality after hepatectomy in patients with fibrosis,[12] as also found in our experimental model (Figure 1C). It is tempting to speculate that massive hepatocyte death at day 5 may directly trigger the progenitor response in our system, which appears to occur via apoptosis (Figure 2D).[29] Interestingly, hepatocyte death was paralleled by an increase in serum TGFβ1 levels in fibrotic mice (Figure 3C), which in contrast was only transiently increased in normal mice at day 1 post-PHx. Because anti-proliferative and pro-apoptotic properties of TGFβ1 in hepatocytes [but not progenitor (oval) cells] are well documented,[30] it is plausible that dysregulation of TGFβ1 may be responsible for the shift from normal hepatocyte-driven regeneration to oval-cell mediated regeneration in fibrotic liver. Further studies are necessary to elucidate the precise molecular mechanism underlying aberrant TGFβ1 responses, hepatocyte death, and the (fibrogenic) progenitor activation during pathophysiological regeneration of the fibrotic liver.

Importantly, we show for the first time that fibrotic liver regeneration is driven mostly progenitor (oval) cell, which is in sharp contrast to mature hepatocyte-mediated regeneration of the normal liver.[1,2,7] Interestingly and unexpectedly, regeneration of fibrotic liver in the late stages (days 3 to 5) was associated with a pronounced increase in several profibrogenic transcripts above levels in active ongoing fibrosis (eg, at the time of surgery that corresponds to peak fibrosis after 6 weeks of CCl₄ treatment), such as TGFβ1, α-SMA, TIMP-1, TGFβ2, and integrin β6.[11] Timing of this severe fibrogenic response coincided with remarkable oval cell activation starting at day 5 (Figure 3B) and was followed by fibrotic matrix deposition around progenitor cell-like ductular proliferations (Figure 4A and Table 2). Progenitors are postulated to give rise to reactive cholangiocytes in chronic liver disease that secrete multiple soluble profibrogenic

factors acting on hepatic stellate cells and myofibroblasts in a paracrine fashion.[11] Moreover, reactive cholangiocytes overexpress integrin αvβ6, which correlates with fibrosis progression in human and experimental liver disease and functionally contributes to progression of experimental biliary liver fibrosis.[20,24] Removal of these activated cholangiocytes via apoptosis is instrumental for biliary fibrosis reversal after surgical restoration of bile flow,[18] further underscoring the important profibrogenic role of the progenitor and cholangiocyte cell lineage.

The functional requirement of a progenitor response for fibrogenesis has not been established to date and is a matter of continued debate.[31] Recent animal studies (albeit descriptive) have questioned the role of the oval cell response in driving fibrosis.[32] Moreover, progenitor cell-mediated regeneration may represent a beneficial compensatory reserve mechanism when normal hepatocyte replication is impaired.[2,33] Therefore, we sought to establish the functional role for the activation of the progenitor (oval) cell compartment during fibrotic liver regeneration by direct manipulation of progenitor cell proliferation after PHx in fibrotic mice. Administration of a TWEAK-blocking monoclonal antibody after hepatectomy efficiently inhibited the progenitor cell response, as expected,[26] and as evidenced by a markedly reduced number of A6-positive cells, inhibition of proliferation marker Ki-67 in ductular cells, and normalized serum ALT levels, and this significantly reduced the profibrogenic response, as reflected by fibrogenic transcript levels (Figure 5 and Table 3). In contrast, administration of the oval cell mitogen recombinant TWEAK-Fc protein[25] post-PHx strongly stimulated progenitor proliferation and the profibrogenic mRNA response in the regenerating liver (Figure 5). TGFβ2, integrin β6, and procollagen α1(I) were most strikingly upregulated, profibrogenic molecules that are associated with reactive cholangiocyte and progenitor-driven fibrogenesis,[19,20,34] further supporting that this was indeed a progenitor cell-driven fibrogenic response. Interestingly, although ductular cell proliferation was suppressed in mice with TWEAK inhibition, the hepatocyte replication rate was significantly increased, shifting the proliferative response

from progenitor-driven to the hepatocyte-driven regeneration (Figure 5C and Table 3). To our knowledge, this is the first direct experimental evidence that hepatic progenitor activation is driving fibrogenesis *in vivo*. This concept was proposed based on early histological observations[35] and later corroborated in correlative studies with human liver samples,[22,23] but thus far lacked functional proof.[31] Although we cannot entirely rule out that TWEAK may act on several cell types in the liver, the most pronounced (and reported *in vivo*) effect of overexpression or exogenous administration of TWEAK is oval cell and progenitor proliferation.[25,26]

In summary, we have established a sequence of pathological events associated with compromised fibrotic liver regeneration. Based on our results, we propose a vicious circle model in which failure of hepatocyte replication and death during fibrotic liver regeneration activates the reserve progenitor (oval) cell compartment, which in turn elicits a severe fibrogenic response and further compromises hepatocyte-mediated liver regeneration in the fibrotic microenvironment. Finally, we demonstrate that therapeutic inhibition of progenitor cell activation via the TWEAK pathway attenuates the fibrogenic response, and improves liver function and regeneration. Therapies that target the progenitor cell may prove to be a novel and promising strategy to improve surgical outcomes in patients with liver fibrosis undergoing PHx.

Acknowledgments

Supplemental Data

Supplemental material for this article can be found at *http://dx.doi.org/10.1016/j.ajpath.2013.03.018*.

References

1. Michalopoulos GK, DeFrances MC: Liver regeneration. Science 1997, 276:60−66
2. Fausto N, Campbell JS: The role of hepatocytes and oval cells in liver regeneration and repopulation. Mech Dev 2003, 120:117−130
3. Roskams TA, Theise ND, Balabaud C, Bhagat G, Bhathal PS, Bioulac-Sage P, Brunt EM, Crawford JM, Crosby HA, Desmet V, Finegold MJ, Geller SA, Gouw AS, Hytiroglou P, Knisely AS, Kojiro M, Lefkowitch JH, Nakanuma Y, Olynyk JK, Park YN, Portmann B, Saxena R, Scheuer PJ, Strain AJ, Thung SN, Wanless IR, West AB: Nomenclature of the finer branches of the biliary tree: canals, ductules, and ductular reactions in human livers. Hepatology 2004, 39: 1739−1745
4. Saxena R, Theise ND, Crawford JM: Microanatomy of the human liver-exploring the hidden interfaces. Hepatology 1999, 30: 1339−1346
5. Sell S: Heterogeneity and plasticity of hepatocyte lineage cells. Hepatology 2001, 33:738−750
6. Roskams T: Different types of liver progenitor cells and their niches. J Hepatol 2006, 45:1−4
7. Malato Y, Naqvi S, Schürmann N, Ng R, Wang B, Zape J, Kay M, Grimm D, Willenbring H: Fate tracing of mature hepatocytes in mouse liver homeostasis and regeneration. J Clin Invest 2011, 121: 4850−4860
8. Shafritz DA, Dabeva MD: Liver stem cells and model systems for liver repopulation. J Hepatol 2002, 36:552−564
9. Hantash BM, Zhao L, Knowles JA, Lorenz HP: Adult and fetal wound healing. Front Biosci 2008, 13:51−61
10. Friedman SL: Mechanisms of hepatic fibrogenesis. Gastroenterology 2008, 134:1655−1669
11. Popov Y, Schuppan D: Targeting liver fibrosis: strategies for development and validation of antifibrotic therapies. Hepatology 2009, 50: 1294−1306
12. Llovet JM, Burroughs A, Bruix J: Hepatocellular carcinoma. Lancet 2003, 362:1907−1917
13. Greene AK, Puder M: Partial hepatectomy in the mouse: technique and perioperative management. J Invest Surg 2003, 16:99−102
14. Popov Y, Sverdlov DY, Sharma AK, Bhaskar KR, Li S, Freitag TL, Lee J, Dieterich W, Melino G, Schuppan D: Tissue transglutaminase does not affect fibrotic matrix stability or regression of liver fibrosis in mice. Gastroenterology 2011, 140:1642−1652
15. Kuramitsu K, Gallo D, Yoon M, Chin BY, Csizmadia E, Hanto DW, Otterbein LE: Carbon monoxide enhances early liver regeneration in mice after hepatectomy. Hepatology 2011, 53:2016−2026
16. Campbell S, Burkly LC, Gao HX, Berman JW, Su L, Browning B, Zheng T, Schiffer L, Michaelson JS, Putterman C: Proinflammatory effects of TWEAK/Fn14 interactions in glomerular mesangial cells. J Immunol 2006, 176:1889−1898
17. Engelhardt NV, Factor VM, Yasova AK, Poltoranina VS, Baranov VN, Lasareva MN: Common antigens of mouse oval and biliary epithelial cells. Expression on newly formed hepatocytes. Differentiation 1990, 45:29−37
18. Popov Y, Sverdlov DY, Bhaskar KR, Sharma AK, Millonig G, Patsenker E, Krahenbuhl S, Krahenbuhl L, Schuppan D: Macrophage-mediated phagocytosis of apoptotic cholangiocytes contributes to reversal of experimental biliary fibrosis. Am J Physiol Gastrointest Liver Physiol 2010, 298:G323−G334
19. Popov Y, Patsenker E, Fickert P, Trauner M, Schuppan D: Mdr2 (Abcb4)-/- mice spontaneously develop severe biliary fibrosis via massive dysregulation of pro- and antifibrogenic genes. J Hepatol 2005, 43:1045−1054
20. Popov Y, Patsenker E, Stickel F, Zaks J, Bhaskar KR, Niedobitek G, Kolb A, Friess H, Schuppan D: Integrin alphavbeta6 is a marker of the progression of biliary and portal liver fibrosis and a novel target for antifibrotic therapies. J Hepatol 2008, 48:453−464
21. Popov Y, Patsenker E, Bauer M, Niedobitek E, Schulze-Krebs A, Schuppan D: Halofuginone induces matrix metalloproteinases in rat hepatic stellate cells via activation of p38 and NFkappaB. J Biol Chem 2006, 281:15090−15098
22. Lowes KN, Brennan BA, Yeoh GC, Olynyk JK: Oval cell numbers in human chronic liver diseases are directly related to disease severity. Am J Pathol 1999, 154:537−541
23. Clouston AD, Powell EE, Walsh MJ, Richardson MM, Demetris AJ, Jonsson JR: Fibrosis correlates with a ductular reaction in hepatitis C:

roles of impaired replication, progenitor cells and steatosis. Hepatology 2005, 41:809−818

24. Patsenker E, Popov Y, Stickel F, Jonczyk A, Goodman SL, Schuppan D: Inhibition of integrin alphavbeta6 on cholangiocytes blocks transforming growth factor-beta activation and retards biliary fibrosis progression. Gastroenterology 2008, 135:660−670

25. Tirnitz-Parker JE, Viebahn CS, Jakubowski A, Klopcic BR, Olynyk JK, Yeoh GC, Knight B: Tumor necrosis factor-like weak inducer of apoptosis is a mitogen for liver progenitor cells. Hepatology 2010, 52:291−302

26. Jakubowski A, Ambrose C, Parr M, Lincecum JM, Wang MZ, Zheng TS, Browning B, Michaelson JS, Baetscher M, Wang B, Bissell DM, Burkly LC: TWEAK induces liver progenitor cell proliferation. J Clin Invest 2005, 115:2330−2340

27. Kato A, Bamba H, Shinohara M, Yamauchi A, Ota S, Kawamoto C, Yoshida Y: Relationship between expression of cyclin D1 and impaired liver regeneration observed in fibrotic or cirrhotic rats. J Gastroenterol Hepatol 2005, 20:1198−1205

28. Xue F, Takahara T, Yata Y, Kuwabara Y, Shinno E, Nonome K, Minemura M, Takahara S, Li X, Yamato E, Watanabe A: Hepatocyte growth factor gene therapy accelerates regeneration in cirrhotic mouse livers after hepatectomy. Gut 2003, 52:694−700

29. Li F, Huang Q, Chen J, Peng Y, Roop DR, Bedford JS, Li CY: Apoptotic cells activate the "phoenix rising" pathway to promote wound healing and tissue regeneration. Sci Signal 2010, 23:ra13

30. Nguyen LN, Furuya MH, Wolfraim LA, Nguyen AP, Holdren MS, Campbell JS, Knight B, Yeoh GC, Fausto N, Parks WT: Transforming growth factor-beta differentially regulates oval cell and hepatocyte proliferation. Hepatology 2007, 45:31−41

31. Clouston AD, Jonsson JR, Powell EE: Hepatic progenitor cell-mediated regeneration and fibrosis: chicken or egg? Hepatology 2009, 49:1424−1426

32. Van Hul NK, Abarca-Quinones J, Sempoux C, Horsmans Y, Leclercq IA: Relation between liver progenitor cell expansion and extracellular matrix deposition in a CDE-induced murine model of chronic liver injury. Hepatology 2009, 49:1625−1635

33. Falkowski O, An HJ, Ianus IA, Chiriboga L, Yee H, West AB, Theise ND: Regeneration of hepatocyte 'buds' in cirrhosis from intrabiliary stem cells. J Hepatol 2003, 39:357−364

34. Milani S, Herbst H, Schuppan D, Stein H, Surrenti C: Transforming growth factors beta 1 and beta 2 are differentially expressed in fibrotic liver disease. Am J Pathol 1991, 139:1221−1229

35. Desmet V, Roskams T, Van Eyken P: Ductular reaction in the liver. Pathol Res Pract 1995, 191:513−524